Electronic Supplementary Material (ESI) for ChemComm.


# Supplementary Information

# Unprecedented highly efficient photoluminescence in a phosphorescent Ag(I) coordination polymer

Haruka Yoshino,*[a] Masaki Saigo,[b] Kiyoshi Miyata,[b] Ken Onda,[b]
Jenny Pirillo,[c] Yuh Hijikata,[c] Wataru Kosaka,[a] and Hitoshi Miyasaka*[a]

[a] *Institute for Materials Research, Tohoku University, 2-1-1 Katahira, Aoba-ku, Sendai 980-8577, Japan. E-mail: haruka.yoshino.a2@tohoku.ac.jp, miyasaka@imr.tohoku.ac.jp*
[b] *Department of Chemistry, Faculty of Science, Kyushu University, 744 Motooka, Nishi-ku, Fukuoka 819-0395, Japan*
[c] *Institute for Chemical Reaction Design and Discovery (WPI-ICReDD), Hokkaido University, Kita 21, Nishi 10, Kita-ku, Sapporo 001-0021, Japan*

*Corresponding author:
Dr. Haruka Yoshino, Prof. Dr. Hitoshi Miyasaka
Institute for Materials Research, Tohoku University, 2–1–1 Katahira, Aoba-ku, Sendai, Miyagi 980-8577, Japan
E-mail: haruka.yoshino.a2@tohoku.ac.jp, miyasaka@imr.tohoku.ac.jp
Tel: +81-22-215-2030
FAX: +81-22-215-2031

**Contents for SI**

## Experimental Section

### Materials

**Warning**: chemicals were purchased from commercial sources and were used without further purification. Cyanide compounds are potentially toxic and should be handled with care and disposed of properly according to local regulations. Even if some cyanide salts have low solubility and might not create significant risks in themselves, they should still be handled with precaution, and their decomposition in strong acids should be avoided.

All chemicals were purchased from commercial sources and used without further purification. $Cd^{II}(pmd)[Ag^{I}(CN)_2]_2$ (**1**; pmd = pyrimidine) was prepared using the following steps.

Single crystals of **1** were prepared using the slow-diffusion method in a straight tube. A solution of $K[Ag(CN)_2]$ (19.9 mg, 0.05 mmol) and pyrimidine (6.01 mg, 0.075 mmol) in $H_2O$ (2.5 mL) was added to a solution of $Cd(NO_3)_2 \cdot 4H_2O$ (15.4 mg, 0.05 mmol) in $H_2O$ (2.5 mL) at room temperature. The solution was allowed to stand for several days and the colourless crystals were obtained. Yield 70.2%. Elemental analysis (%): calculated. for $C_{12}H_8N_8CdAg_2$: C 24.33, H 1.36, N 18.92; found: C 24.30, H 1.42, N 18.82.

### Physical Measurements

Elemental analysis of carbon, hydrogen and nitrogen for $Cd^{II}(pmd)[Ag^{I}(CN)_2]_2$ (**1**; pmd = pyrimidine) was carried out at the Division of the Graduate School of Science, Tohoku University. Scanning electron microscopy (SEM) was conducted using a JEOL JSM-IT200(A) at the Collaborative Research Centre on Energy Materials (E-IMR), Tohoku University (electron high tension (EHT) value:10.00 keV). Infrared (IR) spectra were recorded using a JASCO FT/IR-4200 spectrophotometer with an ATR accessory in the range of 650–4000 $cm^{-1}$ at room temperature (RT). PXRD measurements at RT were performed using a Rigaku Ultima IV spectrometer with graphite-monochromated Cu Kα radiation ($\lambda$ = 1.5418 Å). The variable-temperature synchrotron PXRD data were measured at BL-15 of the SAGA Light Source (SAGA-LS) using a silica glass capillary with an inner diameter of 0.2 mm. ($\lambda$ = 1.08 Å).[1] The sample temperatures were controlled by a dry dinitrogen flow using a Rigaku $GN_2$ apparatus. Thermogravimetric analysis (TGA) was performed at a heating rate of 5 °C $min^{-1}$ using a Shimadzu DTG-60H apparatus under a nitrogen atmosphere. Solid-state UV-visible spectra were collected on a JASCO V-750 spectrometer using a diffuse-reflectance accessory. Variable-temperature emission and excitation spectra were obtained using a JASCO FP-8550 spectrofluorometer with a dual-branch optical fibre and cryostat system (RC102, CRYO Industries). The absolute emission quantum yield was measured using an absolute

emission quantum yield measurement system (Hamamatsu Photonics C9920-02) composed of an integrating sphere, a multichannel photodetector (Hamamatsu Photonics PMA-12), and a 150 W CW xenon lamp as an excitation light source (excitation wavelength = 330 nm) at RT.

The emission quantum yield ($\Phi$) was calculated with the following equation:

$$\phi = \frac{\int I_{em}\, d\lambda}{\int (I_{ex}^{before} - I_{ex}^{after})\, d\lambda}$$

$I_{em}$ is the number of photons, $I^{before}_{ex}$ is the number of photons from the excitation light that is not absorbed, and $I^{after}_{ex}$ is the number of photons from the excitation light that is absorbed.

Photoluminescence lifetimes ($\tau_{em}$) were measured using a streak camera (Hamamatsu C4780) coupled to a polychromator (Acton Research Corporation, SpectraPro-150, spectral resolution: ~10 nm). The detection system was synchronised with a femtosecond Ti:sapphire chirped-pulse amplifier (Spectra-Physics, Spitfire Ace, pulse duration of 120 fs, central wavelength of 800 nm, and repetition rate of 1 kHz). The output of the amplifier was led to an optical parametric amplifier (Light conversion, TOPAS-prime), and the fourth harmonic (350 nm) of the signal pulse (1400 nm) was used as the pump pulse. The polarisation angles of the light for pumping/detection were set to the magic angle (54.7 °) to avoid distortion of the temporal profiles from the molecular orientation.[2] The excitation energy was maintained at less than 0.08 mJ/cm$^2$. The sample temperatures were controlled using a liquid-nitrogen cryostat (UNISOKU, CoolSpeK UV USP-203-B).

The $\tau_{em}$ values were estimated using the following fitting function (single exponential function convoluted with Gaussian as the instrumental response function):

$$f(t) = \int A(t) \cdot B(t-\tau) d\tau \quad \cdots ①$$

$$A(t) = \frac{Amp1}{G_1} * \exp(-G_1 t),\ B(t) = exp\left\{-\left(\frac{t}{pw}\right)^2\right\} \cdots ②$$

$$\begin{aligned} f(t) \ &= \mathrm{A_{const}} \\ &+ \mathrm{A_0} * (1\text{-}\mathrm{erf}(-2 * \sqrt{\ln(2)}/(\mathrm{FWHM} * \sqrt{2}) * \mathrm{t})) \\ &+ \mathrm{A_1} * \exp(-\mathrm{t}/\tau 1) * (1-\mathrm{erf}(-2 * \sqrt{\ln(2)}/(\mathrm{FWHM} * \sqrt{2}) * \mathrm{t})) \quad (\mathrm{t}=\mathrm{x}-\mathrm{t_0}) \quad \cdots ③ \end{aligned}$$

**Single-crystal X-ray diffraction**

Single-crystal X-ray data for **1** at 100, 140, 180, 220, 260, and 300 K were recorded on a Bulker SMART APEX II ULTRA CCD-detector Diffractometer using a rotating-anode (Bruker Tourbo X-ray source) with graphite-monochromated Mo Kα radiation ($\lambda$ = 0.71073 Å) was employed. Data integration and reduction were performed using the APEX2 crystallographic software package and OLEX2 software.[3] A single crystal was mounted on a polymer film with liquid paraffin, and the temperature was kept constant under flowing nitrogen gas. The structure of **1** was solved by a standard direct method (XSHELL V6.3.1 crystallographic software package of the Bruker AXS) and expanded Fourier techniques. All non-disordered and non-hydrogen atoms were refined anisotropically using full-matrix least-squares refinements. All of the hydrogen atoms were placed in the measured positions and refined using a riding model. The relevant crystal data collection and refinement data for the crystal structure of **1** are summarised in **Table S1**.

**Computational analysis**

We optimised the structure **1** at the ground ($S_0$) and triplet ($T_1$) states under periodic boundary condition (PBC) using Crystal17 program,[4,5] referring to the crystal structure of **1** at 300 K. The spin states of all Ag in the unit cell were fixed singlet at $S_0$ and triplet at $T_1$, respectively. We applied pob-TZVP-rev2 basis set [6] for C, H, and N, and pob-TZVP-rev2 with an effective core potential (ECP) [7] for Ag and Cd. PBE functional [8] with Grimme D3 type dispersion correction [9] were employed. The cell parameters were relaxed during the optimisation while maintaining C2/c symmetry. The shrinking parameters were set to 2 and 2.

After optimising **1** at both spin states under PBC, using the optimised crystal structures, the $[Ag_2(CN)_4(pmd)_2]$ unit was modelled, where the pmd ligands were terminated by hydrogen atoms. Only the terminating hydrogen atoms were optimised again to investigate the MOs with M06 functional.[10] For the model calculations at both singlet and triplet states, we employed 6-311G(d,p) for C, H, and N and def2-TZVP with ECP for Ag. All model calculations were performed using Gaussian 16 Rev. C.01.[11]

**Table S1.** Crystallographic data and refinement parameters of **1**.

| *T* / K | 100 K | 140 K | 180 K | 220 K | 260 K | 300 K |
|---|---|---|---|---|---|---|
| CCDC | 2235241 | 2235244 | 2235245 | 2235247 | 2235246 | 2235242 |
| Formula | $C_{12}H_8N_8CdAg_2$ | $C_{12}H_8N_8CdAg_2$ | $C_{12}H_8N_8CdAg_2$ | $C_{12}H_8N_8CdAg_2$ | $C_{12}H_8N_8CdAg_2$ | $C_{12}H_8N_8CdAg_2$ |
| Formula weight | 592.40 | 592.40 | 592.40 | 592.40 | 592.40 | 592.40 |
| Crystal system | Monoclinic | Monoclinic | Monoclinic | Monoclinic | Monoclinic | Monoclinic |
| Space group | *C*2/*c* | *C*2/*c* | *C*2/*c* | *C*2/*c* | *C*2/*c* | *C*2/*c* |
| *a* / Å | 7.1056(8) | 7.1111(7) | 7.1145(7) | 7.1180(7) | 7.1211(6) | 7.1237(9) |
| *b* / Å | 16.1016(18) | 16.1300(15) | 16.1659(16) | 16.1995(17) | 16.2349(13) | 16.274(2) |
| *c* / Å | 14.6696(16) | 14.6487(13) | 14.6332(15) | 14.6181(15) | 14.6055(12) | 14.6035(18) |
| $\alpha$ / ° | 90 | 90 | 90 | 90 | 90 | 90 |
| $\beta$ / ° | 98.1360(10) | 98.0850(10) | 98.0680(10) | 98.0300(10) | 97.9870(10) | 97.9890(10) |
| $\gamma$ / ° | 90 | 90 | 90 | 90 | 90 | 90 |
| *V* / Å$^3$ | 1661.5(3) | 1663.5(3) | 1666.3(3) | 1669.1(3) | 1672.2(2) | 1676.6(4) |
| *Z* | 4 | 4 | 4 | 4 | 4 | 4 |
| $R_1$[a] / % | 1.45 | 1.42 | 2.54 | 2.06 | 1.99 | 1.98 |
| $wR_2$[b] / % | 3.45 | 3.33 | 6.00 | 5.00 | 4.85 | 4.81 |
| Goodness of Fit | 1.031 | 1.058 | 1.037 | 1.120 | 1.143 | 1.141 |

[a] $R_1 = R = \Sigma||F_o|-|F_c||/\Sigma|F_o|$. [b] $wR_2 = [\Sigma w(F_o^2-F_c^2)^2/\Sigma w(F_o^2)^2]^{1/2}$

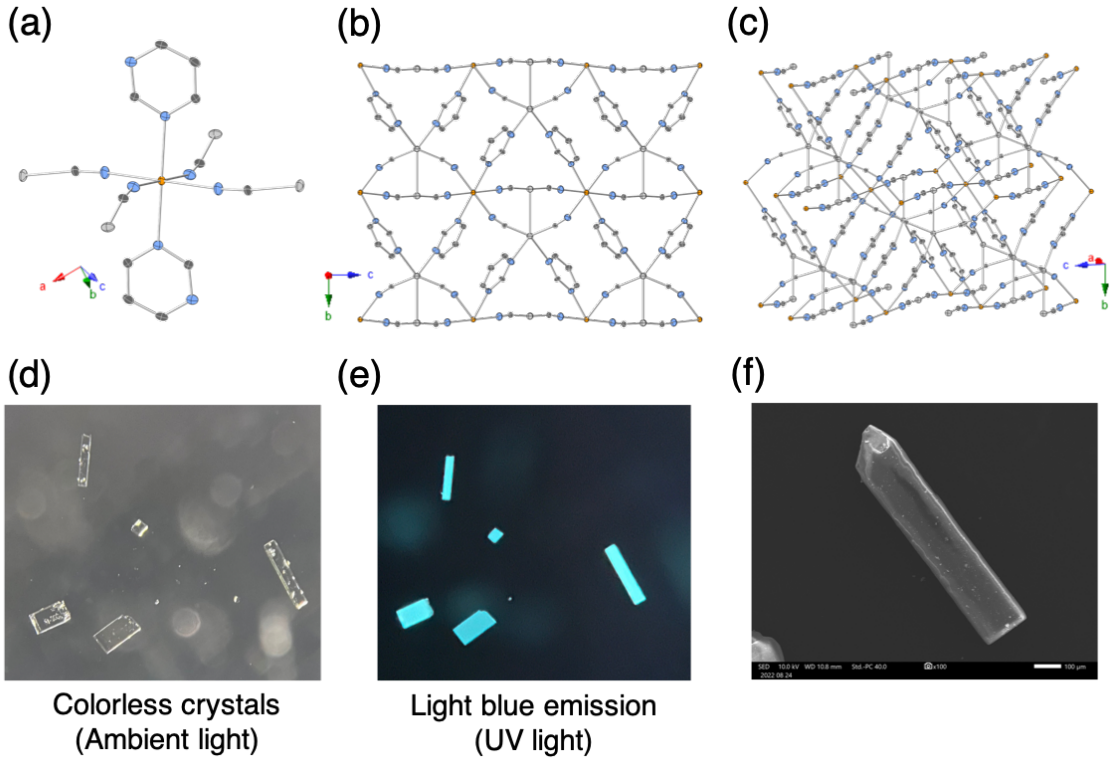


**Fig. S1**. ORTEP drawings of the crystal structure for **1** at 300 K. (a) Coordination environment of Cd site in **1**. (b), (c) Packing structure of **1**. Atomic code: Cd, orange; Ag, light grey; C, grey; N, blue, respectively. H atoms are omitted for clarity. Thermal ellipsoids are shown at the 50% probability level. (d), (e) Photographs of single crystals for **1** under ambient light and UV light ($\lambda_{ex}$ = 365 nm). (f) A scanning electron microscopy (SEM) image of **1** (Electron high tension (EHT) value: 10.00 keV)

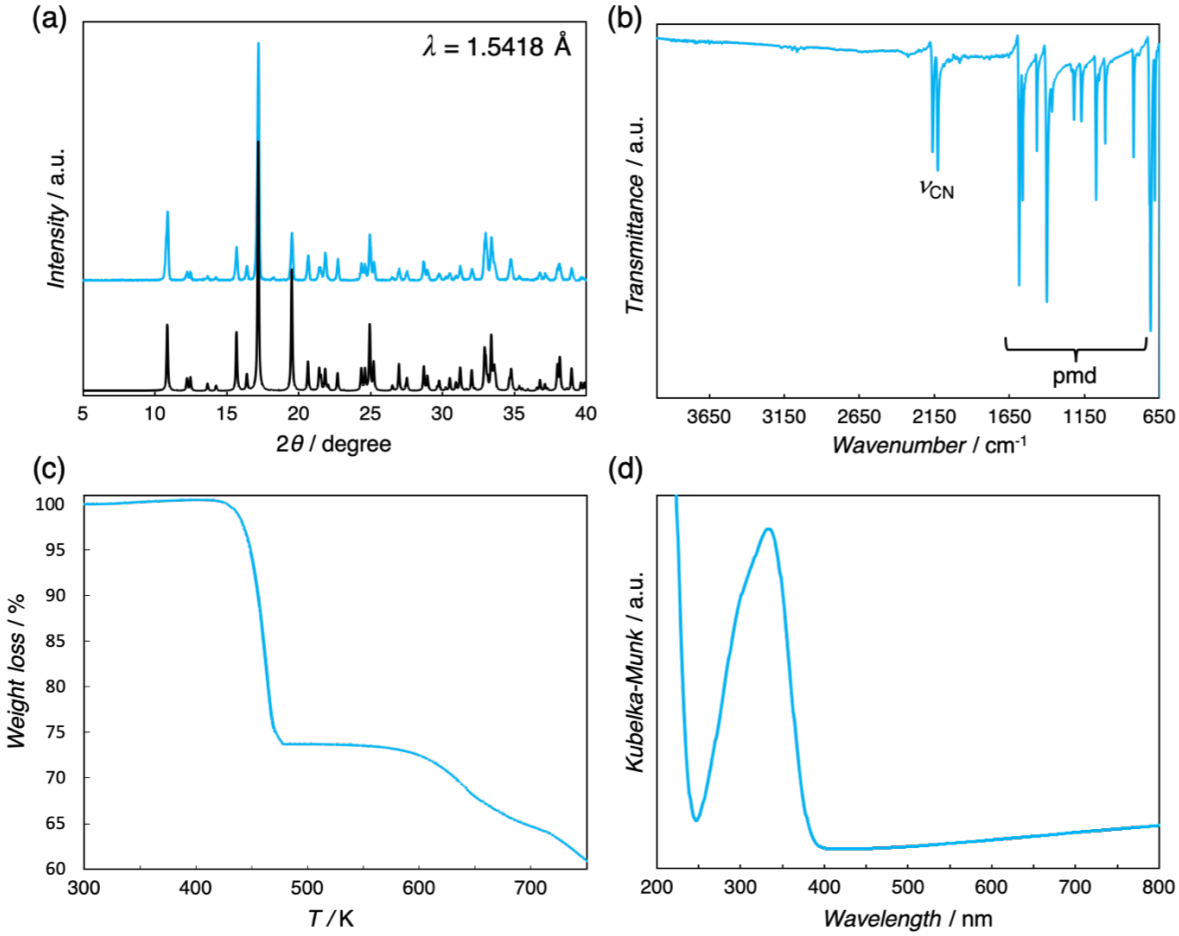


**Fig. S2**. (a) PXRD patterns ($\lambda$ = 1.5418 Å) at RT of **1** (light blue) and simulated pattern (black). (b) IR spectra of **1** at RT. (c) TGA curve of **1** (Heating rate: 5 °C/min under $N_2$ flow). (d) Solid-state UV-vis reflectance spectra of **1** at RT

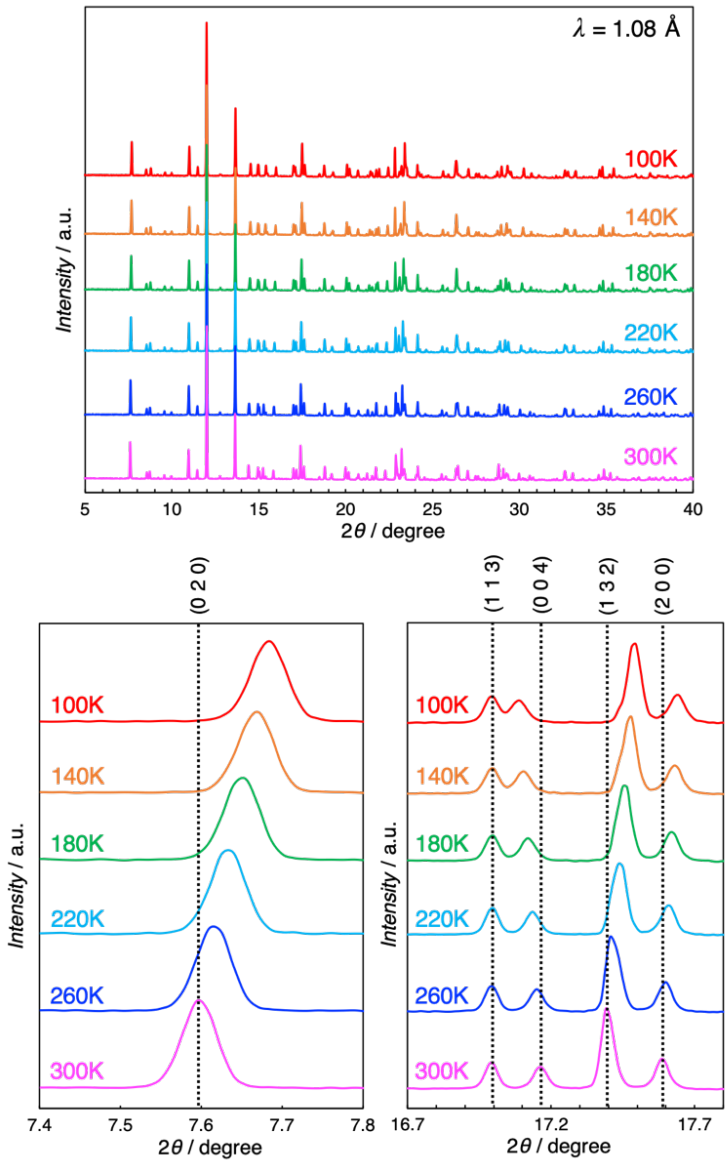


**Fig. S3**. Variable-temperature synchrotron PXRD patterns ($\lambda$ = 1.08 Å) of **1** in the range of 100–300 K

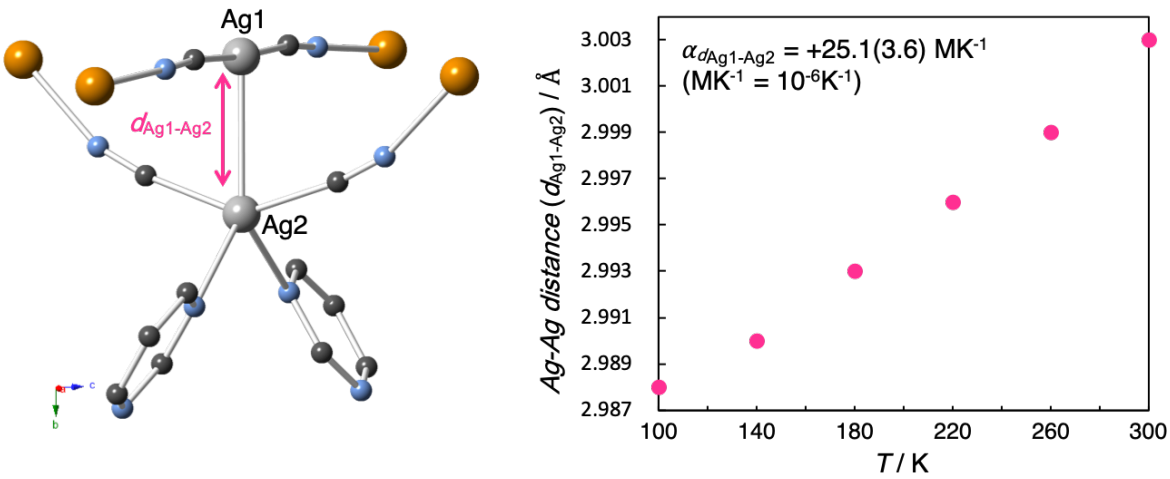


**Fig. S4**. Thermal variation and thermal elongation constants (MK$^{-1}$ = 10$^{-6}$K$^{-1}$) of Ag-Ag distance ($d_{Ag1-Ag2}$), calculated using VT-SCXRD results (100–300 K).

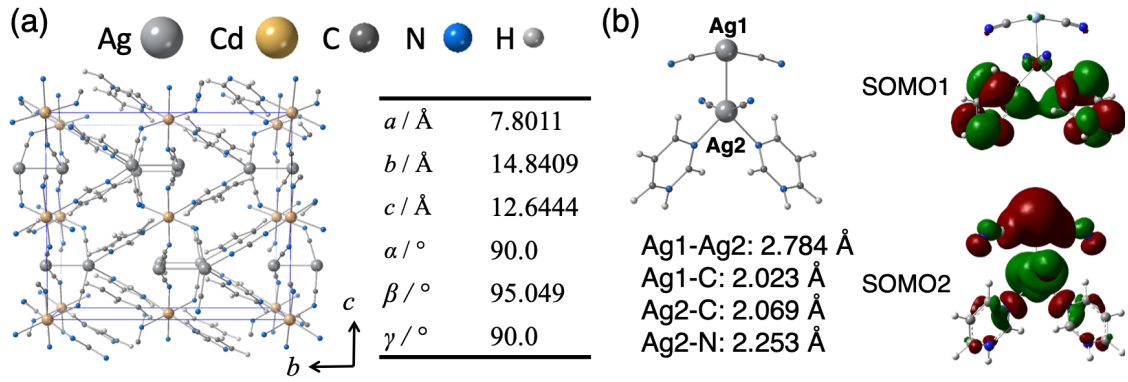


**Fig. S5**. (a) Infinite optimised structure and cell parameters of **1** at the $T_1$ state by DFT calculations. (b) Calculated MOs of model for **1**. SOMO1 and SOMO2 represent the singly occupied highest molecular orbital and singly occupied second highest molecular orbital, respectively.

**Table S2.** Cartesian coordinates of models for a singlet ground state ($S_0$) and a triplet state ($T_1$).

Singlet ground state ($S_0$)

| atom | *x*/Å | *y*/Å | *z*/Å |
|---|---|---|---|
| C | -2.81238300 | 1.99304900 | -0.30639700 |
| C | -0.40041900 | -0.18513000 | -1.98786900 |
| C | 2.79426600 | 1.97846000 | 0.52345300 |
| C | 1.30502900 | 3.27110100 | -0.64691600 |
| C | 2.09258100 | 4.39688700 | -0.42140300 |
| C | 3.24182200 | 4.23349500 | 0.34567300 |
| H | 3.10540100 | 1.00387500 | 0.90450300 |
| H | 0.35679500 | 3.34051500 | -1.18505800 |
| H | 1.80649100 | 5.37464200 | -0.80465500 |
| N | -2.62224500 | 3.14562000 | -0.43795000 |
| N | -0.78127400 | -0.24707500 | -3.10215700 |
| N | 3.58631200 | 3.02183300 | 0.83180800 |
| N | 1.66410800 | 2.04777700 | -0.19179100 |
| H | 3.89195400 | 5.07274100 | 0.60073500 |
| Ag | -2.80373000 | -0.00000100 | 0.00000000 |
| Ag | 0.08736500 | 0.00000000 | 0.00000000 |
| C | -2.81238100 | -1.99305100 | 0.30639800 |
| C | -0.40041900 | 0.18512900 | 1.98786900 |
| C | 2.79426800 | 1.97845800 | -0.52345400 |
| C | 1.30503100 | -3.27110000 | 0.64691700 |
| C | 2.09258400 | -4.39688500 | 0.42140200 |
| C | 3.24182500 | -4.23349300 | -0.34567200 |
| H | 3.10540100 | -1.00387300 | -0.90450400 |
| H | 0.35679700 | -3.34051400 | 1.18505800 |
| H | 1.80649500 | -5.37464100 | 0.80465500 |
| H | 3.89195800 | -5.07273900 | -0.60073500 |
| N | -2.62224300 | -3.14562100 | 0.43795100 |
| N | -0.78127400 | 0.24707500 | 3.10215800 |
| N | 3.58631400 | -3.02183100 | -0.83180800 |
| N | 1.66411000 | -2.04777500 | 0.19179100 |
| H | 4.42018100 | 2.89562500 | 1.39380600 |
| H | 4.42018300 | -2.89562200 | -1.39380500 |

Triplet state ($T_1$)

| atom | *x*/Å | *y*/Å | *z*/Å |
|---|---|---|---|
| C | 2.51197700 | -1.98148300 | -0.25609000 |
| C | 0.33404200 | -0.28732800 | -2.02824000 |
| C | -2.59493200 | -1.45372700 | 0.88939900 |
| C | -1.20174300 | -2.89904200 | -0.38269700 |
| C | -2.12980200 | -3.90795000 | -0.23023000 |
| C | -3.34872400 | -3.64224700 | 0.42796700 |
| H | -2.73754900 | 0.48898300 | -1.37775100 |
| H | -0.23071300 | -3.02802000 | -0.85486700 |
| H | -1.90557700 | -4.90758300 | -0.60678000 |
| H | -4.03505000 | -4.43003600 | 0.73418400 |
| N | 2.21557700 | -3.11355600 | -0.36697000 |
| N | 0.53298400 | -0.54178600 | -3.15919100 |

| | | | |
|---|---|---|---|
| N | -3.50408700 | -2.39739000 | 1.06815500 |
| N | -1.50707100 | -1.62677600 | 0.12159600 |
| Ag | 2.83033600 | 0.00000000 | 0.00000000 |
| Ag | 0.04679000 | 0.00000000 | 0.00000000 |
| C | 2.51197700 | 1.98148300 | 0.25609100 |
| C | 0.33404200 | 0.28732800 | 2.02824000 |
| C | -2.59493200 | 1.45372700 | -0.88939800 |
| C | -1.20174300 | 2.89904300 | 0.38269700 |
| C | -2.12980200 | 3.90795000 | 0.23023000 |
| C | -3.34872400 | 3.64224900 | -0.42796700 |
| H | -2.73754900 | -0.48898200 | 1.37775100 |
| H | -0.23071300 | 3.02802100 | 0.85486700 |
| H | -1.90557700 | 4.90758200 | 0.60678100 |
| H | -4.03505000 | 4.43003800 | -0.73418300 |
| N | 2.21557700 | 3.11355600 | 0.36697000 |
| N | 0.53298400 | 0.54178600 | 3.15919100 |
| N | -3.50408700 | 2.39739000 | -1.06815500 |
| N | -1.50707100 | 1.62677600 | -0.12159600 |
| H | -4.29031900 | -2.24858600 | 1.68794800 |
| H | -4.29031800 | 2.24858600 | -1.68794900 |

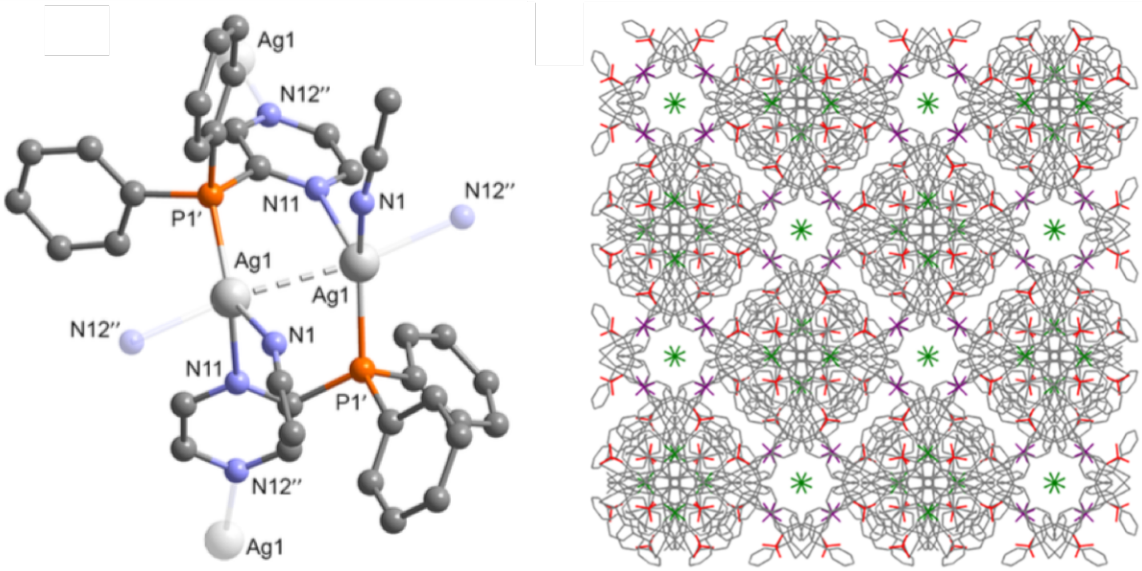


**Fig. S6**. Crystal structure of $\{[Ag_2L_2(CH_3CN)_2](BF_4)_2\}_n$ (**2**; L = diphenyl(2-pyrazyl)phosphine).[12]

## References in SI


1 T. Okajima. Y. Chikaura, M. Tabata, H. Hashimoto, Y. Soejima, K. Hara and N. Hiramatsu, *Nucl. Instr. and Meth. in Phys. Res. B.,* 2005, **238**, 185.

2 R. D. Spencer, G. Weber, *J. Chem. Phys.* 1970, **52**, 1654.

3 O. V. Dolomanov, L. J. Bourhis, R. J. Gildea, J. a. K. Howard and H. Puschmann, *J. Appl. Crystallogr.*, 2009, **42**, 339.

4 R. Dovesi, A. Erba, R. Orlando, C. M. Zicovich-Wilson, B. Civalleri, L. Maschio, M. Rerat, S. Casassa, J. Baima, S. Salustro, B. Kirtman, *WIREs Comput. Mol. Sci*., 2018, **8**, e1360.

5 R. Dovesi, V. R. Saunders, C. Roetti, R. Orlando, C. M. Zicovich-Wilson, F. Pascale, B. Civalleri, K. Doll, N. M. Harrison, I. J. Bush, P. D'Arco, M. Llunell, M. Causà, Y. Noël, L. Maschio, A. Erba, M. Rerat and S. Casassa, CRYSTAL17 User's Manual (University of Torino, Torino, 2017).

6 J. Laun, D. V. Oliveira, T. Bredow, *J. Compt. Chem*., 2018, **39**, 1285.

7 D. V. Oliveira, J. Laun, M. F. Peintinger, T. Bredow, *J. Compt. Chem*., 2019, **40**, 2364.

8 J. P. Perdew, K. Burke, M. Ernzerhof., *Phys. Rev. Lett*., 1996, **77**, 3865.

9 S. Grimme. *J. Comput. Chem*., 2006, **27**, 1787.

10 Y. Zhao, D. G. Truhlar, *Theor. Chem. Acc*., 2008, **120**, 215.

11 Gaussian 16, Revision C.01, M. J. Frisch, G. W. Trucks, H. B. Schlegel, G. E. Scuseria, M. A. Robb, J. R. Cheeseman, G. Scalmani, V. Barone, G. A. Petersson, H. Nakatsuji, X. Li, M. Caricato, A. V. Marenich, J. Bloino, B. G. Janesko, R. Gomperts, B. Mennucci, H. P. Hratchian, J. V. Ortiz, A. F. Izmaylov, J. L. Sonnenberg, D. Williams-Young, F. Ding, F. Lipparini, F. Egidi, J. Goings, B. Peng, A. Petrone, T. Henderson, D. Ranasinghe, V. G. Zakrzewski, J. Gao, N. Rega, G. Zheng, W. Liang, M. Hada, M. Ehara, K. Toyota, R. Fukuda, J. Hasegawa, M. Ishida, T. Nakajima, Y. Honda, O. Kitao, H. Nakai, T. Vreven, K. Throssell, J. A. Montgomery, Jr., J. E. Peralta, F. Ogliaro, M. J. Bearpark, J. J. Heyd, E. N. Brothers, K. N. Kudin, V. N. Staroverov, T. A. Keith, R. Kobayashi, J. Normand, K. Raghavachari, A. P. Rendell, J. C. Burant, S. S. Iyengar, J. Tomasi, M. Cossi, J. M. Millam, M. Klene, C. Adamo, R. Cammi, J. W. Ochterski, R. L. Martin, K. Morokuma, O. Farkas, J. B. Foresman, and D. J. Fox, Gaussian, Inc., Wallingford CT, 2016.

12 M. I. Rogovoy, A. S. Berezin, D. G. Samsonenko and A. V. Artem'ev, *Inorg. Chem.*, 2021, **60**, 6680.